Distributed Phase Plates for Super-Gaussian Focal-Plane Irradiance Profiles

Various phase-plate designs have been investigated to provide different focal-plane irradiation profiles for laser-matter interaction studies. For many interaction experiments it is necessary to (1) achieve a nearly flat super-Gaussian irradiance distribution, (2) minimize scattering losses, and (3) ensure insensitivity to the laser wavefront nonuniformities. This article shows that these goals may be achieved using a distributed phase plate with a strictly continuous surface determined by a new phase-retrieval algorithm.

The first phase-plate designs intended for direct-drive spherical-implosion experiments were two-level plates consisting of an array of discrete rectangular or hexagonal subregions of either 0 or π phase within the region.[1,2] In this case the far-field envelope is defined by the Fourier transform of the subregions and does not conform to a super-Gaussian shape. The lenslet array[3] provides an efficient method of obtaining a flatter irradiation profile; however, it is difficult to control the two-dimensional shape and power spectrum of this profile. Previously designed distributed phase plates (DPP's) with a strictly continuous phase[4] have achieved 96% on-target efficiency but have yielded only a Gaussian[5] or a low-order super-Gaussian far-field distribution. None of these methods provides the desired high-order super-Gaussian shape (see Fig. 63.29) often required for applications in laser-matter interactions.

Phase-retrieval algorithms, developed by Gerchberg and Saxton[6] and Feinup,[7] have been used to synthesize phase plates yielding a higher-order super-Gaussian profile in the far field.[8] We shall refer to this method as phase retrieval with random start (PRRS), as explained below. PRRS is quite general and may be applied to the synthesis of essentially any type of far-field distribution, but we will consider only super-Gaussian distributions in this study. PRRS has no phase discontinuities of magnitude π but exhibits point singularities that cause scattering and line discontinuities of magnitude 2π that can cause scattering as a result of manufacturing errors.

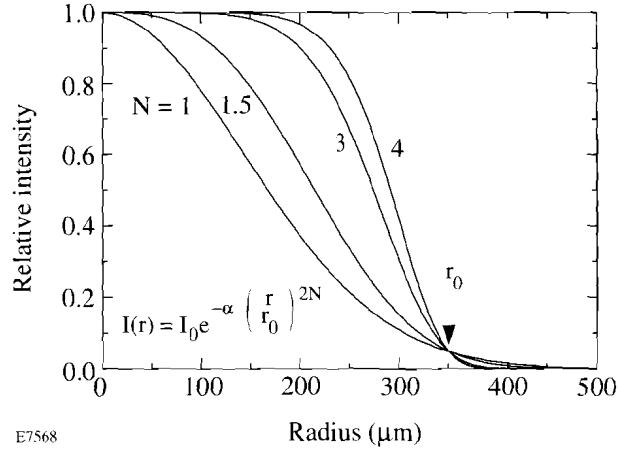

Fig. 63.29
Super-Gaussian irradiance profiles of the form $I(r) = I_0 \exp\left[-\alpha(r/r_0)^{2N}\right]$ for values of N from 1 to 4, plotted with normalized peak irradiances and with α chosen so that all curves pass through 5% of the peak irradiance at the same radius r_0. Energy-normalized profiles would emphasize differences in peak irradiance or beam size. These curves illustrate the relative flatness associated with the higher-order super-Gaussian profiles.

To design a phase plate with the PRRS algorithm, one begins with a random noise distribution (no correlation between neighboring points) in the pupil and then performs four steps iteratively.[7] Figure 63.30 illustrates this process. First, each point in the near-field complex amplitude is normalized to achieve the desired near-field intensity profile, leaving the phase unchanged. Second, the complex amplitude is propagated to the far field. Third, each point in the far-field complex amplitude is normalized to achieve the desired intensity profile while preserving the phase. Fourth, the complex amplitude is propagated back to the near field. These four steps are repeated until the solution converges or the desired level of performance is achieved.

Once the phase-retrieval iteration process is finished, the phase of the complex amplitude distribution in the near field at step 4 determines the surface profile of the phase plate. Synthe-

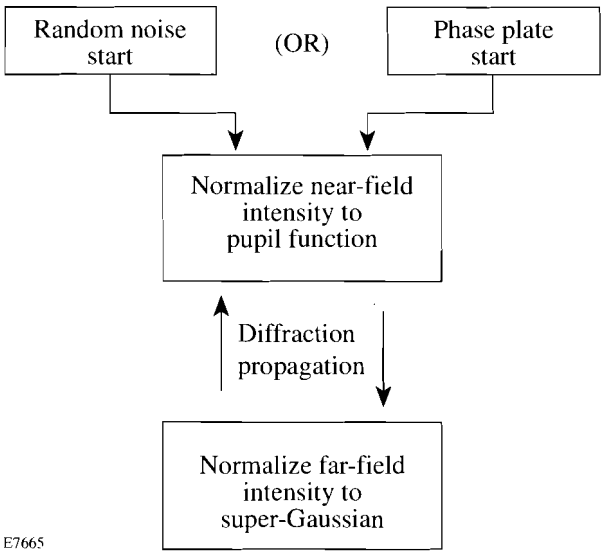

Fig. 63.30
Iterative procedure used to design phase plates according to the phase-retrieval method. Typically, random noise is used in the first pass through the process; however, other phase distributions can be used to reduce the total number of iterations required to achieve an accurate approximation to the desired far-field irradiance envelope.

sis of super-Gaussian far-field profiles by the phase-retrieval algorithm results in speckle-like phase patterns in both the near and far fields. Modulo 2π jumps arise if the range of the phase exceeds 2π because the arctangent function $\Psi = \tan^{-1}(\mathrm{Im}/\mathrm{Re})$ maps the phase into the range $-\pi \le \Psi \le \pi$. The loci of modulo 2π jumps form closed curves. In a kinoform the modulo 2π jumps are left in place; however, phase-unwrapping algorithms can be used to remove these jumps.[9]

Branch cuts are discontinuities of magnitude 2π terminated at each end by a pair of phase poles. Branch cuts, unlike modulo 2π jumps, cannot be phase unwrapped by the elementary unwrapping algorithms because they are line segments rather than closed curves.[9] Figure 63.31 illustrates a positive-negative pole pair with a branch cut between the poles. Phase poles are phase singularities that occur at the point where the loci of real zeros and imaginary zeros cross.[10] Near a phase pole the phase Ψ is a helical function—one cycle of a screw—with a branch cut to constrain $-\pi \le \Psi \le \pi$. The approximate slope of the wavefront in the neighborhood of a circular pole is found by dividing the height of λ by the circumference $2\pi r$, where r is the distance from the pole, giving $\lambda/2\pi r$. This is the source of steep but smoothly varying wavefront slopes, which are a direct source of scattering. The association of wide-angle scattering with the location of poles has been numerically verified by blocking the on-target light in the far field, leaving only the wide-angle scattered light. The resulting distribution is backpropagated to the near field, in which high-intensity spots are found to be coincident with pole locations. Direct scattering occurs at the extreme slopes near poles and at non-2π discontinuities. The 2π line discontinuities should, in theory, cause no scattering; however, they can act as indirect sources of scatter because of finite widths produced by limitations in the manufacturing process.

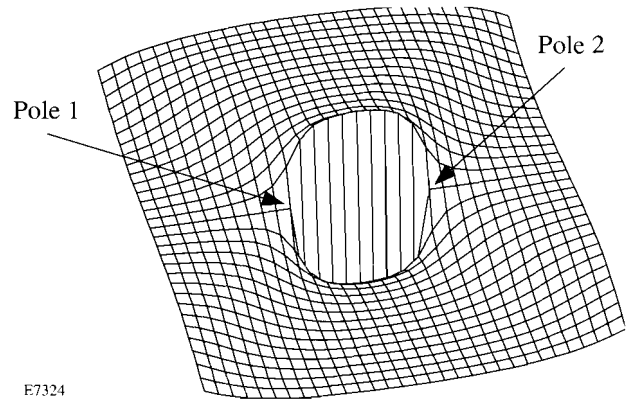

Fig. 63.31
Example of a horizontally oriented pair of positive (right) and negative (left) phase poles with a branch cut between the poles. The wavefront slope in the immediate region of each pole is approximately $\lambda/2\pi r$, where r is the distance from the pole, causing wide-angle vortex scattering. Theoretically the branch cut is a perfectly sharp discontinuity of height λ; however, manufacturing limitations can result in a finite slope to the branch cut, causing scattering loss.

When performing the numerical diffraction calculations of the phase-retrieval algorithm, only the direct source of wide-angle scattering owing to the smooth-surface effects of the vortex phase near poles is observed. The indirect scattering effects of 2π discontinuities are not observed in numerical calculations and may be minimized in the design process either by a reduction of the net length of the discontinuities through phase unwrapping and a reduction in the number of poles or by manufacturing methods that reduce the discontinuity width. For a 0.351-μm wavelength, a 28-cm near-field pupil, a 180-cm focal length, and a 350-μm target radius, PRRS generates ~10,000 poles. Scattering from the vortex surfaces caused a direct scattering loss of ~5%. In this example, wide-angle scattering can be defined as the energy outside a radius of 500 μm. In addition to the 5% scattering loss due to vortex

surfaces, there are additional losses due to the 2π discontinuities: both modulo 2π jumps and branch cuts. If the number of poles can be reduced, then the direct scattering due to vortex surfaces and the indirect scattering due to branch cuts will be reduced.

A strictly continuous phase plate will have negligible scattering loss. Recently a continuous DPP has been developed, using a two-dimensional Fourier grating with random phase to produce a low-order super-Gaussian profile in the far field.[4] For the 60-beam OMEGA laser system, the smallest target radius is 350 μm and the f number is ~6.4. A Fourier grating with a spatial period of 0.49 cm and an amplitude of 0.228 waves (at λ = 351 nm) was used to produce equal far-field modulation for the 0, +1, and −1 orders and generate approximately five major peaks in the far field to form a super-Gaussian envelope. A random phase with an rms value of 0.5 waves and autocorrelation diameter of 0.9 cm was added to the Fourier grating to fill in the gaps between the major peaks of the far field. Figure 63.32 illustrates the far-field patterns from (a) the Fourier grating and (b) a random phase distribution. The GLAD code[11] is used for the DPP design and analysis, in addition to various phase-retrieval algorithms.

The above hybrid DPP design, instead of random noise, was used as a starting point for the phase-retrieval algorithm for the design of the higher-order super-Gaussian DPP.[12] This algorithm is denoted as phase retrieval starting from the hybrid design (PRHD). As indicated in Table 63.I, only 1,400 poles were observed, compared with 10,000 poles for the PRRS. We used only two cycles of phase retrieval since more cycles did not improve the fit to the desired super-Gaussian and resulted in additional poles. Figure 63.33 compares the azimuthally averaged profiles of the desired fourth-order super-Gaussian profile with those produced by the starting hybrid DPP, PRRS, and PRHD, in which an ensemble average based on 100 different noise seeds was used for the random aspects of each design method. The azimuthal average provides strong noise smoothing for larger values of r but no smoothing at $r = 0$. The ensemble average provides additional noise smoothing to display better the shape of the curves at small values of r.

PRHD provides the widest flat region in the center of the target area. As summarized in Table 63.I, the PRRS design has ~5% direct scattering outside the 500-μm radius, compared with 2% for the PRHD design. It is also expected that the indirect scattering that is due to 2π discontinuities will be much lower for the PRHD than the PRRS because there are only 1,400 poles, compared with 10,000 poles, giving a much lower net length of 2π discontinuities, which become important when manufacturing limitations are included.

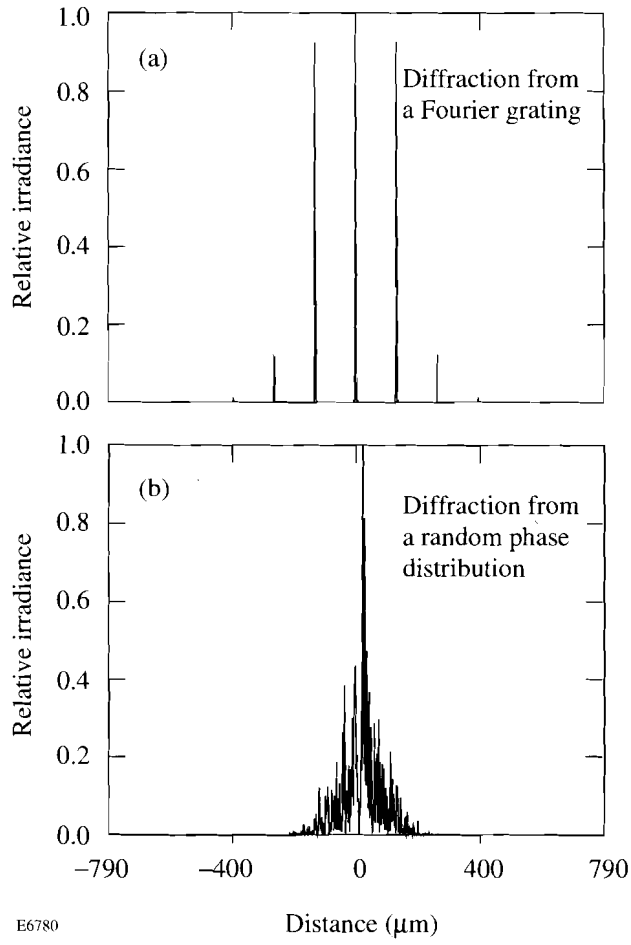

Fig. 63.32
Far-field patterns from (a) a Fourier grating and (b) a random phase distribution used as a starting point for the new phase-retrieval method of designing super-Gaussian DPP's. Since this hybrid DPP produces a far-field irradiance envelope closer to the desired envelope, fewer iterations are required for convergence to the desired super-Gaussian envelope.

Table 63.I: Pole counts and wide-angle scattering losses for the three design types.[(a)]

Phase-plate type	Number of poles	Direct scattering outside 500-μm radius (%)	Approximate super-Gaussian order
PRRS	10,000	5.0	4.0
Hybrid DPP	0	0.3	1.5
PRHD	1,400	2.0	4.0

[(a)] Only direct scattering due to vortices is included in the table.

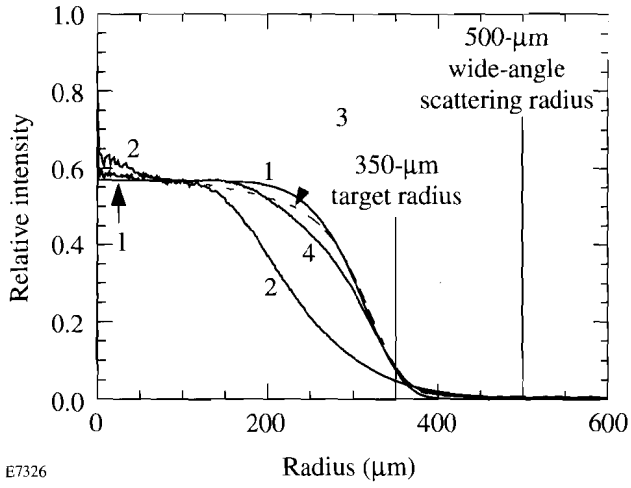

Fig. 63.33
Azimuthally averaged profiles of the fourth-order super-Gaussian function (curve 1), the hybrid DPP (curve 2), the PRRS (curve 3), and the PRHD (curve 4). The curves represent an ensemble average of 100 calculations done with different random seeds. Light that falls outside 500 μm is considered wide-angle scattering. The PRHD has a wider flat region in the center than does the PRRS.

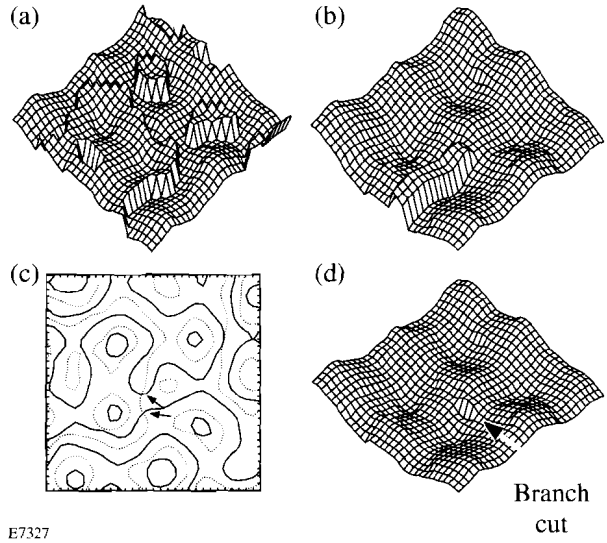

Fig. 63.34
(a) Phase plot of PRHD kinoform showing a 1.2-cm × 1.2-cm section of the 28-cm-diam beam. Islands and plateaus of height λ result in discontinuities of net length ~140 pixel lengths. (b) Conventional phase unwrapping, which ignores branch cuts, reduces the net length of the discontinuities. The phase-unwrapping algorithm fails at the branch cut between the vertically oriented pole pair near the center of the display, creating a spurious horizontal plateau of 28 pixel lengths. (c) Loci of real (solid lines) and imaginary (dotted lines) zeros. The two primary poles are marked. (d) Phase unwrapping with branch-cut recognition reduces the net discontinuity length to the length of the branch cut (approximately two pixel lengths).

Modulo 2π discontinuity scattering, unlike vortex surface scattering, may be reduced by phase unwrapping. Figure 63.34(a) shows a 1.2-cm × 1.2-cm section of the 28-cm-diam aperture with no phase unwrapping and represents the surface if the PRHD were to be implemented as a kinoform. The net discontinuity length for this small section is ~140 pixel lengths. Islands of 2π height are apparent. Figure 63.34(b) shows the result of a conventional phase-unwrapping algorithm that attempts to achieve continuity by first resolving the center column and then resolving the horizontal rows from the center to the left and from the center to the right.[9] The net scattering length is reduced to ~28 pixels. Figure 63.34(c) indicates the pole pair by the crossing of real and imaginary loci. The phase-unwrapping algorithm used in Fig. 63.34(b) did not recognize the branch cut and generated the 13-pixel-long plateau of high phase, seen in Fig. 63.34(c), as a spurious effect. Figure 63.34(d) shows the same small section after correction for the branch cut. The net discontinuity length has been reduced from approximately 140 to 2 pixel lengths.

Summary

A new distributed phase plate that achieves a good approximation to a fourth-order super-Gaussian with very low scattering losses has been designed. Low scattering is achieved because the new design is nearly continuous, having fewer phase poles and a lower net length of 2π phase discontinuities. The net length of 2π discontinuity lines, which in practice are an additional source of scattering because of finite width when manufactured, may be reduced to a low level by a phase-unwrapping algorithm capable of treating branch cuts. Preliminary investigations suggest that even-higher-order super-Gaussian far-field profiles can be generated with this technique.

ACKNOWLEDGMENT

Helpful discussions with Sham Dixit, David Freid, and James Feinup are acknowledged. This work was supported by the U.S. Department of Energy Office of Inertial Confinement Fusion under Cooperative Agreement No. DE-FC03-92SF19460, the University of Rochester, and the New York State Energy Research and Development Authority. The support of DOE does not constitute an endorsement by DOE of the views expressed in this article.

REFERENCES

1. Y. Kato *et al.*, Phys. Rev. Lett. **53**, 1057 (1984).
2. Laboratory for Laser Energetics LLE Review **33**, NTIS document No. DOE/DP40200-65, 1987 (unpublished), p. 1.
3. X. Deng *et al.*, Appl. Opt. **25**, 377 (1986).

4. T. J. Kessler, Y. Lin, J. J. Armstrong, and B. Velazquez, Proc. Soc. Photo-Opt. Instrum. Eng. **1870**, 95 (1993).

5. J. W. Goodman, in *Laser Speckle and Related Phenomena*, Springer Series in Applied Physics, Vol. 9, edited by J. C. Dainty (Springer-Verlag, Berlin, 1984), Chap. 2, p. 9.

6. R. W. Gerchberg and W. O. Saxton, OPTIK **35**, 237 (1972).

7. J. R. Fienup, Appl. Opt. **21**, 2758 (1982).

8. S. N. Dixit *et al.*, Opt. Lett. **19**, 417 (1994).

9. J. M. Huntley, Appl. Opt. **28**, 3268 (1989).

10. B. Ya. Zel'dovich, N. F. Pilipetsky, and V. V. Shkunov, in *Principles of Phase Conjugation*, Springer Series in Optical Sciences, Vol. 42, edited by T. Tamir (Springer-Verlag, Berlin, 1985), p. 79.

11. GLAD is a general purpose laser system and physical-optics computer program. It is a proprietary product of Applied Optics Research, Tucson, AZ.

12. Y. Lin, T. J. Kessler, and G. N. Lawrence, Opt. Lett. **20**, 764 (1995).